Available online at www.sciencedirect.com
SCIENCE DIRECT®
C. R. Geoscience 336 (2004) 281–290
COMPTES RENDUS GEOSCIENCE

Tectonics

Kinematics of the Corinth Gulf inferred from calcite dating and syntectonic sedimentary characteristics

Christiane Causse [a,*], Isabelle Moretti [b], Rémy Eschard [b], Luca Micarelli [b], Bassam Ghaleb [c], Norbert Frank [d]

[a] *Laboratoire de Moulis, CNRS (FRET 2576), 09200 Saint-Girons, France*
[b] *Institut français du pétrole, 1 et 4, av. de Bois-Préau, 92852 Rueil-Malmaison cedex, France*
[c] *GEOTOP, UQAM, av. du Président-Kennedy, H3C3P8 Montréal, Québec, Canada*
[d] *LSCE, Domaine du CNRS, bât. 12, 91198 Gif-sur-Yvette cedex, France*

Received 12 November 2003; accepted after revision 24 November 2003

Written on invitation of the Editorial Board

Abstract

New data on faults from the western-central area of the Corinth Gulf give new insights into the kinematics of this rift zone. The Xylokastro Fault was active 1 Myr ago and also around 108 ka. The Doumena Fault is younger than the Pirgaki Fault, so out-of-sequence, and was active 125 ka ago. Cements from two faults sampled on the northern coast have given two ages, respectively close to 300–400 ka and greater than 1 Myr. These new data confirm the recent fault activity on the two rift borders. ***To cite this article: C. Causse et al., C. R. Geoscience 336 (2004).***

Résumé

Cinématique du golfe de Corinthe basée sur la datation des ciments calcitiques de failles et les caractéristiques des dépôts syntectoniques. De nouvelles datations sur les failles et fractures du centre-ouest du golfe de Corinthe permettent de préciser la cinématique de la zone. La faille de Xylokastro a enregistré des rejets il y a environ 1 Ma et autour de 108 ka. La faille de Doumena est postérieure à la faille de Pirgaki, donc *out-of-sequence*, et a joué il y a 125 ka. Les deux failles datées sur la côte nord ont respectivement des âges de l'ordre de 300–400 ka et supérieurs à 1 Ma. Ces données confirment l'activité sub-actuelle des failles sur les deux bordures du rift. ***Pour citer cet article : C. Causse et al., C. R. Geoscience 336 (2004).***

Keywords: Normal faulting; Greece; Corinth Rift; Th/U dating

Mots-clés : Faille normale ; Grèce ; Rift de Corinthe ; Datation Th/U

* Corresponding author.
E-mail address: causse@lsm.cnrs.fr (C. Causse).

1631-0713/$ – see front matter
doi:10.1016/j.crte.2003.11.017

Version française abrégée

1. Introduction

Les phases majeures de l'évolution du golfe de Corinthe ont été décrites par Ori [10] et se divisent en un protogolfe qui a pu débuter dès le Miocène et le rift actuel pliocène. De nombreux auteurs s'accordent désormais à penser que le rift actuel s'est développé depuis environ 1 Ma [9,12,14]. Pour cette dernière phase, les difficultés de datation des sédiments syn-rift ont laissé ouvertes certaines discussions sur la cinématique de la zone. Dans ce travail, nous avons employé la méthode de datation U/Th sur les ciments calcitiques des failles et fractures actives du golfe de Corinthe pour valider un modèle cinématique.

2. Échantillonnage, méthode et analyse

Sur l'ensemble des plans de faille affleurant dans le golfe de Corinthe, seul un petit nombre présente des ciments de calcite pure adaptée à la datation Th/U (Fig. 1). En effet, un certain nombre ne contient pas de remplissage de calcite et d'autres, comme la faille d'Helike, ont une gouge centrale principalement formée d'éléments de l'encaissant, dans laquelle aucune veine néoformée ne peut pratiquement être isolée. Nous avons néanmoins trouvé 23 échantillons apparemment susceptibles de mesures d'âges. Les résultats de l'analyse de 15 échantillons sont présentés ici, leur position est reportée sur la Fig. 1, leur description dans le Tableau 1 et les âges obtenus ainsi que les teneurs en radioéléments dans le Tableau 2. Le déséquilibre $^{230}Th/^{234}U/^{238}U$ permet d'obtenir des âges valides dans un matériau contenant de l'uranium et pas de thorium au moment de sa cristallisation, ce qui est le cas des cristaux, et notamment de la calcite, formés à partir d'une solution, puisque l'uranium seul, de ces deux éléments, est soluble [6]. L'éventuelle présence de ^{232}Th dans des calcites contenant des argiles, par exemple, signe la présence initiale de ^{230}Th et nécessite une correction de l'âge calculé [2]. La mesure par TIMS (*Thermo-Ionisation Mass Spectrometry*) de ce déséquilibre permet de déterminer des âges jusqu'à 600 ka. Nous avons limité les analyses aux échantillons contenant plus de 50 ppb d'uranium, afin que la taille requise des échantillons reste faible (2 à 4 g) et puisse être obtenue en minimisant les risques de mélange entre calcite néoformée et encaissant. Les données U–Th et les âges obtenus sont présentés sur les Figs. 2 et 3.

3. Discussion et conclusion

Deux failles ont été échantillonnées sur la côte nord du golfe, à l'est d'Itea (Fig. 1). La faille près d'Itéa est plus ancienne que 1 Ma. Les veines de calcite de la faille nord–ouest située dans la péninsule ont un âge compris entre 300 et 400 ka. Cette nouvelle donnée confirme l'activité de cette faille durant la phase de *rifting* actuelle. L'activité des failles normales à pendage sud qui affectent la côte nord du golfe de Corinthe a été décrite par de nombreux auteurs [9, 11,13], bien qu'elle ait été minimisée dans certains modèles [1,12].

Sur la faille de Xylocastro, deux âges ont été trouvés dans deux veines différentes : l'une d'elles indique un âge compris entre 600 ka et 1 Ma, et l'autre un âge proche de 110 ka. Bien que d'autres échantillonnages soient nécessaires pour affirmer ou infirmer la reprise des déplacements sur la faille de Xylocastro entre ces deux âges, ces résultats suggèrent une cinématique de la faille de Xylocastro similaire à celle publiée pour la faille de Pirgaki [8] : jeu dès le début de la phase actuelle de *rifting*, il y a environ 1 Ma, et reprise (ou accélération) du rejeu durant les derniers 120 ka ; ces failles sont toujours actives.

La faille de Douména est située au sud de la faille de Pirgaki (Fig. 1). L'analyse des faciès sédimentaires du syn-rift dans le voisinage montre que cette faille est tardive : elle est postérieure à tous les dépôts sédimentaires qui affleurent à proximité et les décale. Ces dépôts de type cône alluvial représentent pour nous la partie proximale des grands deltas déposés plus au nord, au-delà de la faille de Pirgaki. L'âge de 125 ka trouvé pour les calcites cimentant la faille de Doumena conforte cette analyse des faciès sédimentaires : la faille apparaît clairement comme tardive, *out of sequence*, par rapport à un modèle simple de propagation vers le nord, tel qu'il a été proposé [3,12], et contemporaine de la faille d'Helike.

Ces nombreux âges de calcites autour de 125 ka suggèrent une accélération dans la cinétique du golfe. L'apparition de la faille d'Aigion il y a environ 50 ka [8] et les datations de certaines veines proches de la

faille d'Helike à la même époque indiquent que cette phase se prolonge actuellement. Elle est identifiable comme une 3e phase dans la propagation du rift telle qu'elle a été décrite par certains auteurs [7,9].

1. Introduction

The evolution of the Gulf of Corinth is often described as a two-phase process with a slow first phase and a fast second one from Late Pliocene to now [10]. Other authors propose a simple tectonic history of the Corinth Rift as a continuous sequence from 900 ka to present time with a progressive migration of the tectonic activity from south to north [12]. New field observations and dating of calcite cements collected from various faults allow us to present a more complex scenario. Our field study is focussed on the western part of the Corinth Rift from Xylocastro to Aigion (Fig. 1). The normal faults, which have a general east–west trending, are dipping to the north and are present from Kalabrita to the centre of the gulf [9]. The first synrift deposits are now uplifted in the northern Peloponnese, which underwent a strong uplift during the last 1 Myr.

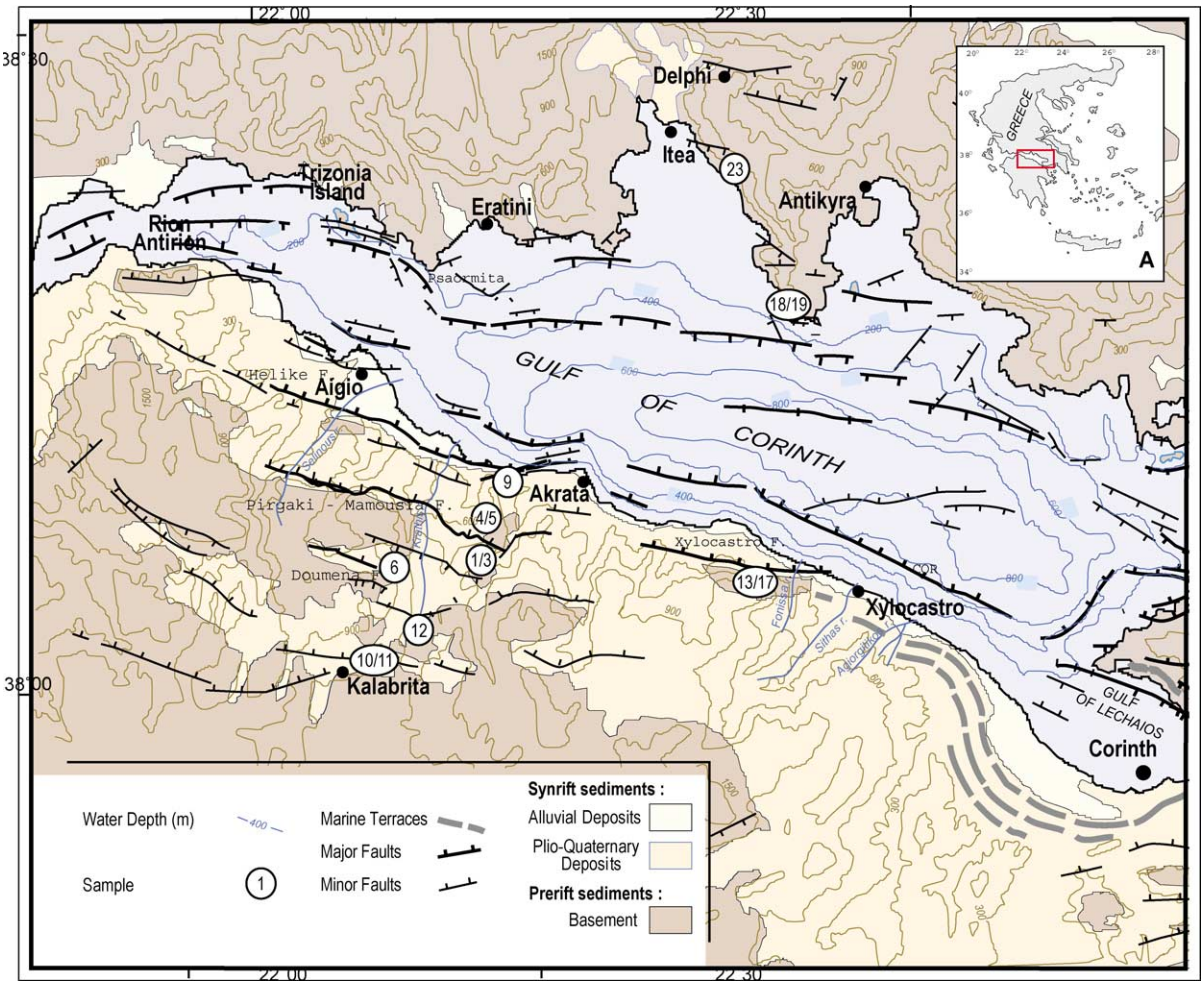

Fig. 1. Structural map of the Corinth Rift, showing sampling locations (modified from [5,9,14]).

Fig. 1. Carte structurale du golfe de Corinthe, indiquant la localisation des échantillons (modifiée d'après [5,9,14]).

Classically, the fault appearance is dated by the first syn-tectonic deposit, but in the Gulf of Corinth a large part of the syn-rift deposit is poorly dated; therefore, we decided to approach the dating of the fault by measurement of the Th/U disequilibrium of calcite cements collected on plane faults. Thermo-Ionisation Mass Spectrometry (TIMS) measurements were performed on calcite containing at least 50 ppb of uranium in order to limit the sample size (2 to 4 g) to ensure proper selection of pure cement and avoid calcareous fragments of host rocks.

2. Sampling strategy

Among plane faults, only few contain pure calcite cements suitable for Th/U dating. Indeed, a large part of the fault zones shows no cement at all, whereas others show calcareous breccias dominantly composed of fragments of host rocks with very thin and discontinuous calcite veins that are practically impossible to isolate, and the last unsuitable category shows a complete mixture of new cement and detrital material coming from host rock.

In order to get a more precise picture of the kinematics of the area rather than the time lapse of a specific fault activity, we sampled as many faults as possible in the western part of the Gulf, from both southern and northern shores. The map in Fig. 1 shows the location of the analysed samples.

3. Samples location and description

Faults and samples description and location are summarised in Table 1.

Samples could be divided into three groups:

(i) major faults, Doumena and Xylokastro (samples #6, and #13 to #17),
(ii) minor faults (on the southern shore, samples #4, #5, on the northern shore, samples #18, #19, #23),
(iii) fractures and minor faults intra synrift deposits (samples, #1 to #3, #9 and #10 to #12).

Microstructures of all thin sections were observed in order to check crystalline fabric of calcite, eventual mixing of different phases, stylolitic figures indicating pressure effect related to tectonism. Except two samples (#9 and #18) chosen in spite of their poor crystalline appearance, but considered as highly significant for tectonic studies, calcite cements were generally made of pure white calcite sometimes automorphous. Only a few of them have clearly shown tectonic influence (#5, #16, #17) marked by stylolitic fabric and/or very variable size grain.

4. Th/U analyses on calcite cements

Because Th is practically insoluble under natural conditions and U is highly soluble, a time-dependent disequilibrium may form between these two elements, which makes some samples datable by means of measuring $^{230}Th/^{234}U/^{238}U$ disequilibria. To obtain a valid date with these data, some prerequisite conditions have to be satisfied:

(i) at crystallisation time (zero time or initial time) the sample contains only uranium and no thorium,
(ii) the geochemical system remains closed after crystallisation, i.e., no migration of uranium has occurred after crystallisation (see [6] for a review).

In such a favourable case, there is no ^{232}Th, and U content, as well as the $^{234}U/^{238}U$ ratio, are constant in one geological unit. For calcite cements collected from fault planes of the studied area, these two conditions were satisfied when we analysed only true calcareous cement, crystallised from a liquid phase, no matter if they were of surficial or deep origin. While doing it, we avoided mixture with detrital material from host rocks, and selected calcite cements characterised by a high degree of crystallisation resulting in a non-porous calcite, making the secondary percolation by a fluid phase impossible. As fault planes are impermeable, the assumption of closed system conditions with respect to uranium for calcite cements seems reasonable. An additional proof may be found through consistent results obtained for sub-samples cut from the same calcite cement.

The presence of ^{232}Th would mean a mixture with detrital material containing all U-series isotopes and particularly initial ^{230}Th, not produced in situ. For such samples, the age calculation needs a correction

for this so-called excess thorium, through the knowledge of initial $^{230}Th/^{232}Th$ [2]. Corrected so, the ages are assumed valid if the correction effect is limited, for $^{230}Th/^{232}Th$ ratios greater than 20, or if the correction introduces age differences lower than the error bar, expressed, as usually, by the 2σ counting statistics [6].

From 18 fault planes sampled for Th/U dating (Fig. 1 and Table 1) when their calcite cements look suitable for this dating method, i.e., apparently made of pure white and non-porous calcite, we obtained only 13 measurable ages for various reasons (Table 2).

Table 1
Faults and samples location and description

Tableau 1
Description et localisation des échantillons et des failles

Sample #	Site description	Sample description
1, 2, 3	Road from Akrata to Tsivlos Lake 37°56′–22°19′5″ Veins in a syn-rift conglomeratic sequence. S0 N20–60° W	Well-crystallised pure calcite with large parallel crystals. Smaller crystals close to the conglomerate. No tectonism effect on crystallic fabric, no stylolitic fissure, breaks through some crystals never pass grain limits.
4	Road from Kato Potamia to Voutsimos 38°07′51″–22°15′27″ Vein 170–10° E	Same crystallisation as above.
5	Road from Kato Potamia to Voutsimos 38°07′51″–22°15′27″ Vein 70–80° S	Stylolitic fissures and many fluid inclusions are visible on a white well crystallised calcite.
6	Doumena Fault, southwest from Doumena Village 38°06′04″–22°07′42.3″ Main fault plane contact Cretaceous carbonate/synrift N86–56° N Striae 84° E	Well-crystallised white calcite showing thin laminar growing, looking like a flowstone passing to a thin and dense crystalline fabric.
9	Road from Platanos to Kalamias Vertical open fracture reaching the present surface	Multi-layered cement symmetrically deposited on the fracture walls, poorly crystallised, detrital material abundant.
10, 11	Main road one km North Kalabrita	Flowstone (10) grown in a fractured conglomerate and stalagmite (11) grown over it. Pure white calcite without tectonic marks.
12	Road Kalabrita–Diakofto, crossing road to Doumena Fracture in synrift conglomerate N110–60° N	Small flowstone covering a fracture wall in a conglomerate. Pure white calcite without tectonic marks.
13, 14, 15	Xylokastro Fault Ano Loutro N80–67° N	Automorphous calcites on fault plane.
16	Xylokastro Fault About 500 m south from Ano Loutro	Fibrous calcite typical of flowstones. Microstructure shown one stylolitic figure, normal to the long axis fibres, due to tectonism.
17	Fracture in the foot wall of Xylokastro Fault at a few metres from the main fault plane ; same site as sample 16	Crystalline fabric is strongly affected by tectonism. Grain size is highly variable, stylolitic fissures are abundant and large, normally cutting the length axis of the major number of crystals.
18	Northern shore. Main fault plane N100 70° S 38°17′10.8″–22°33′53.9″	Poorly crystallised carbonaceous cement, multi-layered, containing detrital material.
19	Same site 50 m southward	Pure white calcite of a single generation fabric, with smaller crystal surrounding breccia fragments.
23	Northern shore, near Itea Normal fault 110°55 S	Highly variable size grain could reflect a multi-generation fabric of pure white calcite.

Table 2
U and Th data of calcite cements. All data are measured by TIMS, ages are calculated using Ludwig half-times. The isotopic dilution method was done using a spike calibrated with HU1 standard uraninite. Repeated analyses ($N = 10$) of HU1 yield respective mean values of 1.0026 and 1.0015, with reproducibility (2σ) of 0.0050 and 0.0066 for $^{234}U/^{238}U$ and $^{230}Th/^{234}U$ activity ratios. When secular equilibrium is reached for both ratios ($^{230}Th/^{234}U$ and $^{234}U/^{238}U$), a lower limit of age equal to 1 Ma can be assumed (sample #23). If only $^{234}U/^{238}U$ is out of equilibrium, it means an age lower than the time necessary to reset the secular equilibrium for this ratio. The initial value for this ratio being unknown, an age calculation is impossible, but considering the $^{234}U/^{238}U$ values in this area, we suggest an age lower than 1 Ma (sample #17). Correction for Th-excess, using the hypothesis of an initial $^{230}Th/^{232}Th$ ratio equal to 1, was only needed for samples #9b and #12a (A_1 are corrected ages)

Tableau 2
Données U–Th des ciments calcitiques. Les données sont mesurées par TIMS, les âges sont calculés en utilisant les périodes de Ludwig. La dilution isotopique a été réalisée avec un traceur calibré par rapport à l'uraninite standard HU1 supposée à l'équilibre. La réplication ($N = 10$) des analyses de HU1 a donné des valeurs moyennes respectivement égales à 1,0026 ($2\sigma = 0{,}0050$) et 1,0015 ($2\sigma = 0{,}0066$) pour $^{234}U/^{238}U$ et $^{230}Th/^{234}U$. Quand les deux rapports d'activité ($^{230}Th/^{234}U$ et $^{234}U/^{238}U$) sont à l'équilibre, on ne peut indiquer qu'une limite inférieure de l'âge (âge > 1 Ma pour l'échantillon #23). Si $^{234}U/^{238}U$ est seul hors équilibre, l'âge est au-delà de la limite (> 600 ka) et inférieur à la durée de remise à l'équilibre de ce rapport, soit un âge inférieur à 1 Ma, compte tenu des rapports obtenus dans les calcites du golfe de Corinthe (échantillon #17). Une correction du thorium initial, utilisant l'hypothèse d'un rapport initial $^{230}Th/^{232}Th$ égal à 1, a été nécessaire pour les échantillons #9b et #12a

Sample #	^{238}U (ppm)	2σ	$^{234}U/^{238}U$ AR	2σ	$^{230}Th/^{234}U$ AR	2σ	$^{230}Th/^{232}Th$ AR	2σ	Age (ka)	2σ	U (ppb) ICPMS
1a	0.0862	0.0001	1.351	0.012	1.061	0.013	237	3	380	+45/–32	55–96
2	0.0691	0.0003	1.445	0.011	1.018	0.011	170	2	289	+15/–13	87
3	0.0846	0.0003	1.436	0.010	1.002	0.026	123	3	274	+31/–25	55
4	0.0430	0.0001	1.318	0.020	1.093	0.019	38	0.3	561	+643/–133	121
6a	0.0613	0.0001	1.537	0.011	0.719	0.013	281	4	124.3	±3	55
6b	0.0703	0.0001	1.512	0.013	0.762	0.067	1326	100	138.3	+23/–19	72
9b	0.6235	0.0012	1.039	0.007	0.436	0.005	31	0.4	62(A_0) 50(A_1)	±0.7	407
12a	0.0485	0.0002	1.231	0.012	0.335	0.034	3.5	0.7	43(A_0) 35(A_1)	±5	45
16a	0.887	0.006	2.123	0.004	0.698	0.002	140	1	112.3	±0.4	871
16b	0.549	0.001	2.131	0.009	0.681	0.005	208	2	108.2	±0.9	642
17b	0.0425	0.0002	1.023	0.009	1.001	0.016	57	1	$\geqslant 600$ & < 1000	nd	37
17c	0.0880	0.0004	1.021	0.008	1.041	0.031	333	10	$\geqslant 600$ & < 1000	nd	47
18	0.2576	0.0002	1.303	0.005	1.124	0.011	58	1	U leaching	nd	230–319
19	0.0497	0.0001	1.068	0.009	0.985	0.016	210	4	360	+67/–41	49
23	0.1018	0.0005	1.001	0.010	1.013	0.031	59	2	> 1000	nd	93

The major reason is the U content of calcite. The first U–Th measurements on calcite cements from the Corinth Rift faults have shown large variations for U contents: around 1 ppm to a few ppb. These latter samples were unsuitable for dating, because the size sample needed to ensure a precise selection of the pure cement would be too large. Another reason is the existence of excess thorium, only interpretable as a result of U leaching after crystallisation. Additionally, some samples are found to be close to, or have reached, the limit of the method.

Considering that three grams are a minimum weight to obtain ages as young as 40 ka for a sample containing 50 ppb of uranium, it would be impossible to control cleanliness in terms of pure calcite of large enough samples to get an age with a 5 ppb U content calcite. In order to avoid unusable tedious chemical preparations, we first checked U content through ICPMS measurements. When measured by TIMS, ICPMS measurements were generally found in agreement (Table 2). We observed a continuous variation from 5 ppb up to 800 ppb. We retained 40 ppb as a practical threshold of sample suitability for Th/U dating. The lowest U contents were found for samples containing noticeable Th amounts. Consequently, these samples showed Th/U mass ratios greater than 1 (samples #10 to #15). When two or three sub-samples were isolated from calcite cement, they showed comparable values arguing for a homogeneous composition and a probable single generation. The time gap of around 4 ka for sub-samples **a** and **b** of sample #16 does not argue for distinct generations.

On the northern coast, sample #18 did not give an age, because $^{230}Th/^{234}U$ showed a default of uranium due to a probable U leaching after deposition despite a high residual U content. This could explain one of the rare U content variations (230 and 319 ppb) shown by ICPMS analyses (Table 2, Fig. 2). This sample was made of a multi-layered cement not well crystallised. On the same fault area, sample #19, made of white calcite cementing a fault breccia, gave an age of about 360 ka (+67/–41 ka as 2σ). Close to Itea, one sample,

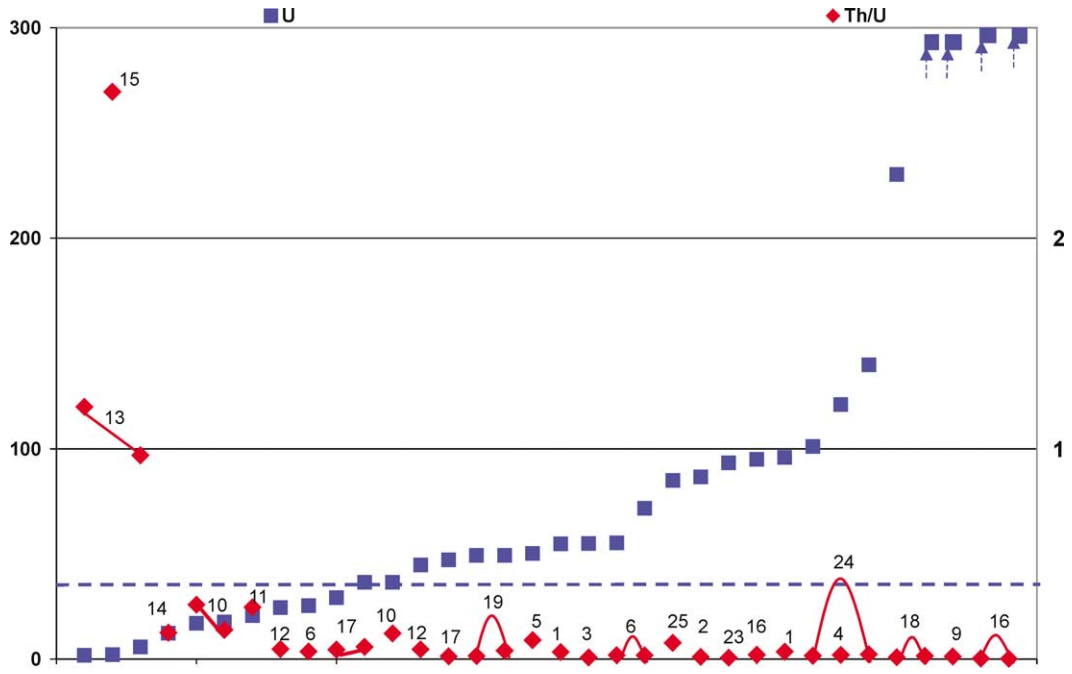

Fig. 2. Uranium content and Th/U mass ratio (U content and Th/U mass ratio determined by ICPMS measurements). Samples are ordered following increasing U content. Sub-samples of the same cement are line-linked, showing the general homogeneous composition of these calcite cements.

Fig. 2. Teneurs en uranium et rapports de masse Th/U (mesures par ICPMS). Les échantillons sont ordonnés par teneur croissante en uranium. Les sous-échantillons prélevés sur un même ciment calcitique sont identifiés de façon à souligner leur homogénéité.

made of an 'apparently' young calcite, showed that the $^{230}Th/^{234}U$ and $^{234}U/^{238}U$ activity ratios were equilibrated, which demonstrates that the age is above the upper limit of the method, i.e., greater than the time necessary to reset equilibrium between ^{234}U and ^{238}U, which means more than one million years.

On the southern coast, breaks cutting conglomerates of synrift deposits, south of the Pirgaki Fault, are filled with large calcite crystals samples (#1–3). Sample #1 gave an old age comprised between 350 and 425 ka, within a 2σ interval. Samples #2 and #3 gave also old ages respectively attributed to 276–304 ka and 269–305 ka within 2σ interval. The same conclusion of an old age may be applied to sample #4 in spite of a low precision of the age determination. We propose to retain a minimum age of 430 ka. This calcite cement filled a minor fault in calcareous sediments parallel to the major Pirgaki Fault.

Two samples collected on the Xylokastro Fault gave highly different ages, respectively old ($\geqslant$600 ka but $<$1000 ka) and young (around 110 ka). Two sub-samples #17 showed $^{230}Th/^{234}U$ activity ratios at secular equilibrium, taking into account the error bars, and $^{234}U/^{238}U$ activity ratios characterised by an excess of daughter isotope. ^{234}U excess is not important, but it is clearly out of equilibrium. These results demonstrate that ages are comprised between the durations necessary to reach the respective secular equilibrium of these two ratios. We retain ages comprised between 600 and 1000 ka. On the same fault, a multi-layered sample, made of a fibrous calcite around 4-cm thick covering a fracture in calcareous host rock (sample #16) was also analysed twice. The U content was the most elevated in this area, as well as $^{234}U/^{238}U$ activity ratios. Only a minor correction has to be made for Th-excess; the two layers analysed gave coherent ages around 110 ka with a time lag of about 4 ka between the two analysed layers. This sample also reported by Flotté et al. [4] was classified as post-tectonism by these authors. But microstructures observed through thin sections for all samples rarely shown stylolitic figures, except for the two samples collected on this fault.

Another sample undoubtedly crystallised very soon after a tectonic phase on the Doumena Fault (sample #6), made of pure white calcite filling a 2 cm void between fault walls, gave also a young age from two analyses of two sub-samples. The U content is not very high (less than 100 ppb) and the $^{234}U/^{238}U$ activity ratios are rather elevated, around the same value close to 1.5. The age determination around 124 ka ($\pm$3 ka, as 2σ) obtained for sub-sample #6a is confirmed also with a lower precision by the result given by sub-sample #6b.

A multi-layered calcareous deposit fills a fracture affecting syn-rift deposits close to Helike Fault. We analysed the sub-sample (#9b) apparently more suitable for the U–Th measurements: the elevated U content and low detrital material (pure white layer). The calculated age is equal to 62 ka and 50 ka after correction for Th-excess. These data have to be considered as indicative of a young age, without more precision because of a large correction due to ^{232}Th abundance meaning that this carbonate is not pure, but mixed with detrital material, inferring a questionable real amount of in situ ^{230}Th. It should also be noticed that this layer is apparently porous as well as other layers, poorly arguing for closed system conditions.

The youngest sample of this sampling is dated around 35 ka. This age determination is not precise, as a lot of detrital material mixed with the calcite resulted in a high ^{232}Th amount and a low $^{230}Th/^{232}Th$ ratio equal to 3.5, implying a non-negligible correction for excess thorium. Nevertheless, this sample is obviously young, 50 ka being an upper age limit and 35 ka is not very far from the true age of this calcite deposited in a recently opened fracture.

5. Discussion and conclusion

The precise kinematic of the Gulf of Corinth is still widely debated due to the lack of dates. Our measurements, therefore, allow us to precise the central/western gulf evolution. The age distribution of the analysed samples is presented in Fig. 3.

The two samples on the northern shore indicate (1) an age older than 1 Myr for a fault with a large offset located at the level of Itea and (2) 3–400 000 yr for the normal fault on the Peninsula southeast from the previous fault. This second fault has an offset of more than 50 m. These two dates indicate that these faults are synchronous of the faults on the southern shore. They constitute another evidence of the fault activity along the northern shore of the Gulf of Corinth already emphasised by marine data [9,13] and by

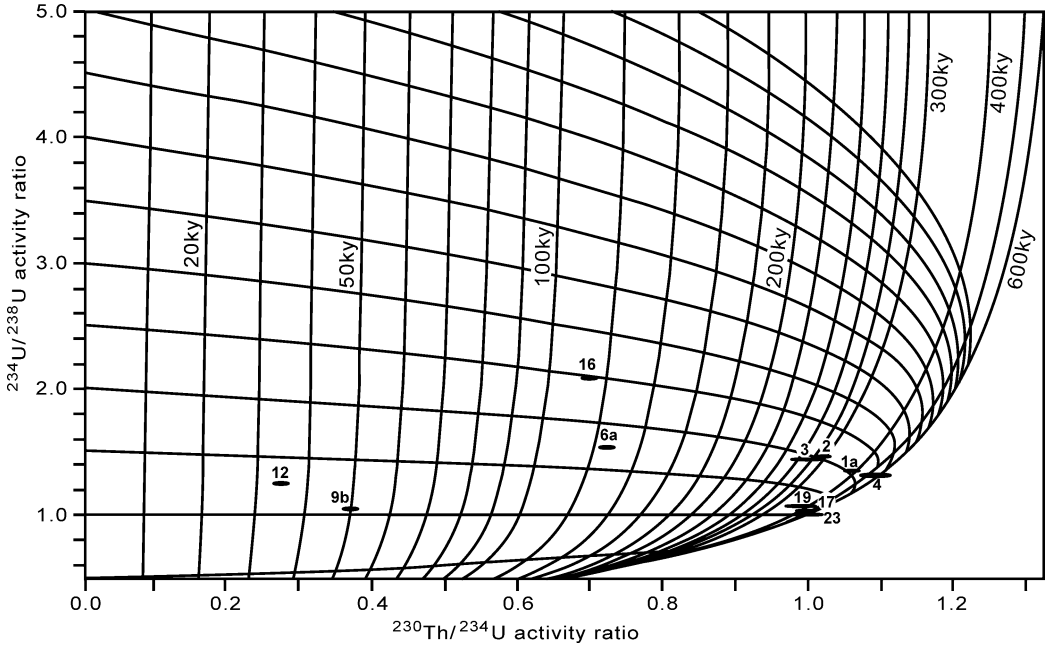

Fig. 3. Age distribution of the analysed samples, showing the increase of uncertainty for the ages close to the 600-ka age limit.
Fig. 3. Distribution des âges obtenus. On remarque l'augmentation des erreurs en termes d'âge pour les âges proches de 600 ka.

archaeological evidences [11], although minimised by some authors.

On the southern shore, two ages have been determined for the Xylocastro Fault: one between 0.6 and 1 Myr and the other at about 110 000 yr (this second dating has also been published in [4]). One may note that in the Mamousia–Pirgaki Fault, located westward but more or less in the prolongation of the Xylocastro Fault, Micarelli et al. [8] have evidenced a polyphasic evolution by means of structural analyses. The first phase cannot be dated yet on the Pirgaki Fault, but is 'old', since at least 3 km of sediments have been eroded from this time. The second phase is contemporaneous of the Gilbert type fan delta deposit (between 1.2 and 0.9 Myr, [9]) and the 2001 seismic event proved than the system is still (or again) active [15]. The veins in the fault where we collected sample #4, a fault parallel to the Mamousi–Pirgaki fault located just northward of the main fault plane, have been dated at 430 000 yr as a minimum age. This result suggests that the Pirgaki Fault System had undergone a continuous activity during the last Myr.

The Doumena Fault is located southward from the Pirgaki–Mamousia fault system. The outcrop, south of the Doumena town, exposes an impressive east–west fault plane formed by numerous shear planes with variable dips (from 45° to 65° N). The footwall consists of the Mesozoic carbonates and the hangingwall of synrift deposits. These deposits are part of a fan delta that could be an internal part of the delta situated northward from the Pirgaki Fault. On the opposite, the Pirgaki–Mamousia System clearly affects the synrift deposits, the Gilbert delta growth above the through created by the Pirgaki fault offset. The Doumena Fault does not affect the sedimentation of the exposed layers on its hanging wall in term of grain size and pebble content. On the opposite, the existence of structural features, such as drag and hangingwall syncline, also suggests that the fault has affected the synrift sequence and their deposits, and thus postdates it. The date (125 ka) given by our results confirms this out-of-sequence position of the Doumena Fault, as compared to a simple northward-propagation model proposed by [3,12]. At this stage of our knowledge we cannot precise the appearance of the Doumena Fault, the fan delta is not directly dated, but we consider it as contemporaneous of the Gilbert type delta. In this hypothesis, the Doumena Fault is younger than

0.9 Myr and our new dates have proven that it was active 125 000 years ago. It means that during the same period 120 000 ± 10 000 yr, the Helike Fault appeared, the Xylocastro Fault has been reactivated and the Doumena Fault has been active. All these data suggest an increase of the tectonic activity in the Gulf during the last 125 000 yr. Based on the analysis of onshore and offshore data, Moretti et al. [9] and Lykousis et al. [7] have highlighted this activity and proposed the identification of a third tectonic phase in the Gulf of Corinth's evolution. They consider that the main feature of this phase is the uplift of the Peloponnese that triggers reactivation of oldest faults and the appearance of new ones.

The other two sites of dating were in minor faults, fractures and veins through the synrift deposits. Samples #1, #2 and #3 gave ages between 0.3 and 0.4 Myr. The structural importance of these intra-post rift sediment faults is weak, but the calcite clearly post-dated the sediments, which are therefore older than 400 000 years.

In the location where we collected sample #9, the veins affect the syn-rift sediment uplifted on the footwall of the Helike Fault. The outcrop is located just a few hundred metres southward from the Helike Fault. The veins have been dated at around 50 ka. This age is the same as that of the Aigion fault appearance [8] and confirms the continuation of the current kinematic phase.

Acknowledgements

This study has been funded by the EEC (Vth PCRD) through the project 3F-Corinth (ENK6-CT-2000-00056)), J. Schuppers being the scientific adviser. We are very grateful to Francesca Ghisetti and her colleagues, Livio Vezanni and Rick Sibson, who made the structural map of the Aigion area and with whom a part of the sampling has been carried out.

References

[1] R. Armijo, B. Meyer, G.C.P. King, A. Rigo, D. Papanastassiou, Quarternary evolution of the Corinth Rift and its implications for the Late Cenozoic evolution of the Aegean, Geophys. J. Int. 126 (1996) 11–53.

[2] C. Causse, J.-S. Vincent, Th/U disequilibrium dating of Middle and Late Pleistocene wood and shells from Banks and Victoria Islands, Arctic Canada, Canad. J. Earth Sci. 26 (1989) 2718–2723.

[3] N. Flotté, D. Sorel, Structural cross section through the Corinth–Patras detachment fault-system in the northern Peloponnesus (Aegean arc, Greece), Proc. 9th Int. Congr. Geol. Soc. Greece, Athens, September 2001, Bull. Geol. Soc. Greece 34 (1) (2001) 235–241.

[4] N. Flotté, V. Plagnes, D. Sorel, A. Benedicto, Attemps to date Pleistocene normal faults of the Corinth–Patras Rift (Greece) by U/Th method and tectonic implication, Geophys. Res. Lett. 28 (19) (2001) 3769–3772.

[5] F.C. Ghisetti, L. Vezzani, F. Agosta, R. Sibson, I. Moretti, Tectonic setting and sedimentary evolution of the south–west margin of the Corinth Rift (Aigion–Xylocastro area), IFP Report No. 562 11, 2001.

[6] M. Ivanovich, A.G. Latham, T.L. Ku, Uranium-series disequilibrium, applications in geochronology, in: M. Ivanovich, R.S. Harmon (Eds.), Uranium Series Disequilibrium: Applications to Earth, Marine and Environmental Sciences, Oxford University Press, Oxford, 1992, pp. 513–552.

[7] V. Lykousis, D. Sakellariou, I. Moretti, H. Kaberi, Late Quaternary basin evolution of the Gulf of Corinth: sequence stratigraphy, sedimentation, fault-slip and subsidence rates, Mar. Geol., submitted for publication.

[8] L. Micarelli, I. Moretti, J.-M. Daniel, Influence of depth and amount of displacement of the characteristics of normal faults, case study in the Gulf of Corinth, Greece, J. Geodyn. 36 (2003) 275–303.

[9] I. Moretti, D. Sakellariou, V. Lykousis, L. Micarelli, The Gulf of Corinth: An active half graben?, J. Geodyn. 36 (2003) 323–340.

[10] G.G. Ori, Geologic history of the extensional basin of the Gulf of Corinth? (Miocene-Pleistocene), Greece, Geology 17 (1989) 918–921.

[11] L. Piccardi, Active faulting at Dlephi, Greece: seismotectonic remarks and a hypothesis for the geologic environment of a myth, Geology 28 (7) (2000) 651–654.

[12] D. Sorel, A Pleistocene and still-active detachment fault and the origin of the Corinth–Patras rift [Greece], Geology 28 (1) (2000) 83–86.

[13] A. Stefatos, G. Papatheodorou, G. Ferentinos, M. Leeder, R. Collier, Seismic reflection imaging of active offshore faults in the gulf of Corinth, their seismotectonic significance, Basin Res. 14 (4) (2002) 487–500.

[14] R. Westaway, The Quaternary evolution of the Gulf of Corinth, central Greece: coupling between surface processes and flow in the lower continental crust, Tectonophysics 348 (2002) 269–318.

[15] J. Zahradnik, J. Jansky, E. Sokos, A. Serpetsidaki, H. Lyon-Caen, P. Papadimitriou, Modeling the $Ml = 4.7$ mainshock of the February–July 2001 earthquake sequence in Aegion, Greece, J. Seismol, submitted for publication.